ESKİŞEHİR TECHNICAL UNIVERSITY JOURNAL OF SCIENCE AND TECHNOLOGY
A- APPLIED SCIENCES AND ENGINEERING

Estuscience – Se, 2025, 26 (3) pp. 188 -202, DOI: 10.18038/estubtda.1624326

RESEARCH ARTICLE

AN EXPERIMENTAL–THEORETICAL INSIGHT INTO SYNTHESIS AND OPTICAL PROPERTIES OF STRUCTURALLY TUNED II-CONJUGATED SCHIFF BASES

Sultan Funda EKTİ [1, *], Handan Can SAKARYA [2], Yunuscan SİVRİKAYA [3]

[1] Department of Chemistry, Faculty of Science, Eskişehir Technical University, Eskişehir, Turkey
sfekti@eskisehir.edu.tr - 0000-0001-6810-0030

[2] Department of Chemistry, Faculty of Science, Eskişehir Osmangazi University, Eskişehir, Turkey
hsakarya@ogu.edu.tr - 0000-0001-8174-1350

[1] Graduate School of Natural and Applied Sciences, Department of Chemistry, Eskişehir Osmangazi University, Eskişehir, Turkey
yunuscansivrikaya@gmail.com - 0000-0001-7158-3205

Abstract

Novel Schiff bases 3a, 3b, and 3c were synthesized, and their optical properties were investigated through experimental methods focusing on the determination of optical band gaps (Eg) derived from UV/Vis absorption spectra. These compounds are identified as N-(6-methylbenzo[d]thiazol-2-yl)-1-(pyren-1-yl)methanimine (3a), 1-(anthracen-9-yl)-N-(6-methylbenzo[d]thiazol-2-yl)methanimine (3b), and 1-(9H-fluoren-2-yl)-N-(6-methylbenzo[d]thiazol-2-yl)methanimine (3c). To reveal the key structural and optical characteristics of these molecules, theoretical calculations were performed using Density Functional Theory (DFT) and Time-Dependent DFT (TD-DFT) at the B3LYP/6–31G(d,p) level. Theoretical results were compared with experimental data to comprehensively evaluate molecular geometries, UV/Vis spectroscopic parameters, and frontier molecular orbital (FMO) energy levels. Nonlinear optical (NLO) properties were analyzed in relation to molecular structure, substitution patterns, conjugation length, and intramolecular charge transfer (ICT) characteristics. The calculated first-order hyperpolarizability (β) values for compounds 3a, 3b, and 3c in DMSO were found to be 4379.6, 7261.4, and 7434.4 a.u., respectively, approximately 110, 183, and 187 times higher than that of the standard reference compound urea. These findings indicate that the synthesized Schiff bases are promising candidates for future applications in photonics and optoelectronics.

Keywords

Schiff base,
NLO,
Hyperpolarizability,
Optical properties,
DFT

Time Scale of Article

Received : 03 February 2025
Accepted : 13 July 2025
Online date : 25 September 2025

1. INTRODUCTION

The nonlinear optical (NLO) properties of materials are essential, since comprehending and leveraging these attributes can significantly improve the efficacy of diverse photonic and optoelectronic systems. Investigations into these features have resulted in the creation of novel materials, encompassing organic [1][2], inorganic [3], organometallic [4] and nanoparticles [5-8], all of which exhibit promise for nonlinear optical applications in photonics and optoelectronics. Organic materials, particularly, frequently possess benefits over inorganic counterparts owing to their remarkable thermal, mechanical, and chemical capabilities, rendering them excellent options for organic optical materials. [9-11]

*Corresponding Author: sfekti@eskisehir.edu.tr

Delocalized conjugated π electrons in organic compounds interact with strong electromagnetic fields such as molecular lasers, causing polarization. This interaction enhances the delocalization within the π-conjugation that connects electron-donating and electron-withdrawing groups, making the organic material more appealing. Organic compounds that feature azomethine (-N=CH-) as a conjugated π-linkage are leading candidates in optical and NLO material research. This is due to their efficient and cost-effective synthesis compared to other π-linkers. Schiff bases, also known as azomethines, are obtained from the reaction of aldehydes and amines. Schiff base compounds hold significant importance and intrigue due to their diverse biological activities. They demonstrate strong antipyretic, antiproliferative, antibacterial, antifungal, anticancer, and antiviral properties, making them valuable subjects for research in the development of novel therapeutic agents. [12-14]. Moreover, these remarkable compounds reveal both linear and nonlinear optical characteristics [14-19], making them of great interest in various fields. This paper presents the synthesis of three novel Schiff bases **3a**, **3b**, and **3c**, whose structures were precisely described by ^{1}H NMR, ^{13}C NMR, ESI-MS, and elemental analysis. The UV-visible spectroscopy technique was used to examine the optical characteristics of compounds **3a-3c**. According to the literature, the band gap energies of these compounds were ascertained using UV-visible absorption spectrophotometry [20] [21].

Density Functional Theory (DFT) is widely utilized in theoretical research to assess molecular geometries, vibrational frequencies, and electronic properties. According to the Runge-Gross theorem, Time-Dependent Density Functional Theory (TDDFT) [22] expands DFT to tackle time-dependent issues. It provides an accurate formulation of time-dependent quantum mechanics. TDDFT has become a valuable method for obtaining precise and reliable predictions of excited-state properties in linear and nonlinear systems.

In computer-aided chemical calculations of Schiff bases, the B3LYP method and the 6-31 G (d,p) basis set are primarily chosen because of their compatibility with experimental data [23,24]. This study employed DFT and TD-DFT calculations to conduct conformational analysis, obtain thermodynamic data, and investigate the optical properties of newly developed Schiff bases [25, 26].

2. RESULTS AND DISCUSSION

Figure 1 delineates the synthesis pathway to the desired Schiff base analogues. Compounds **3a**, **3b**, and **3c** were synthesised using the general method, and spectroscopic techniques were used to determine their structures. The FT-IR spectra of compounds **3a**, **3b**, and **3c** do not exhibit peaks at 3400 cm^{-1}, which are indicative of the amino group present in 6-methyl-2-amino benzothiazole. Furthermore, there are no observable peaks at 1745 cm^{-1}, corresponding to the C=O group characteristic of aldehydes. The azomethine group of chemical 4 is indicated at 1586 cm^{-1}. Additional peaks were recorded at 3010 cm^{-1} (aromatic C-H), 2910-2853 cm^{-1} (aliphatic C-H), 1561 cm^{-1}, 1531 cm^{-1}, and 1480 cm^{-1} (C=C peaks) (Figure S1). The FT-IR spectra of compounds **3b** and **3c** exhibit signals analogous to those observed in the FT-IR spectrum of compound **3a** (Figures S2 and S3).

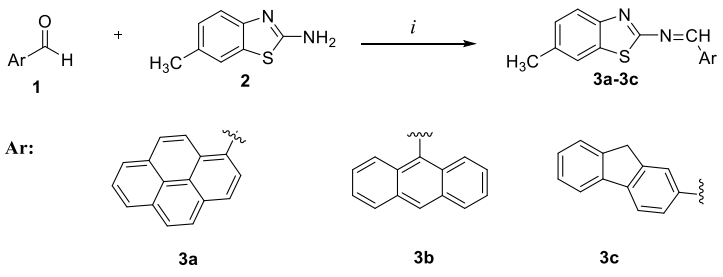

i: *EtOH , 5% HCl, 75^{o}C, reflux, N_2*

Figure 1. Synthesis route of novel synthesized **3a**, **3b**, and **3c**

According to ^{1}H NMR spectra of compound **3a** (Figure. S4), signals corresponding to three distinct protons of the benzothiazole and nine protons of the pyrene have been detected within the 7.34 to 9.26 ppm range. Compound **3a**'s π electrons are conjugated with the azomethine group, which functions as a donor group, effectively directing the ring electrons towards the benzothiazole ring (see Figure 2). Consequently, protons in the pyrene ring are not exposed to conjugated π electrons as seen in the resonance structures of the compound. As a result, it was observed in the lower area compared to the chemical shift value of the protons in the benzothiazole ring. The electron density surrounding the H17 and H10 protons is reduced due to resonance effects. The protons under consideration are positioned closer to the azomethine group (-CH=N-) in comparison to the other protons within the pyrene ring. Consequently, these protons resonate at lower chemical shifts, specifically at 9.29 ppm and 8.84 ppm, corresponding to the H10 and H17 protons, respectively. Additional protons associated with pyrene are detected at8.43 (H11, H13, H14, and H9), 8.39 (H16), 8.28 (H15), 8.16 (H12), 7.86 (H5 and H7) and 7.34 (H14) ppm, respectively. Since the benzothiazole ring is the acceptor, its proton resonance was observed at 7.86 (H5 and H7) and 7.34 (H4) ppm. The literature indicates that the azomethine proton in the Schiff base resonated at around 8-9 ppm, whereas the azomethine proton -(CH=N-) was noted at 10.03 ppm due to the resonance delocalization of the donor π-electrons from the pyrene ring.

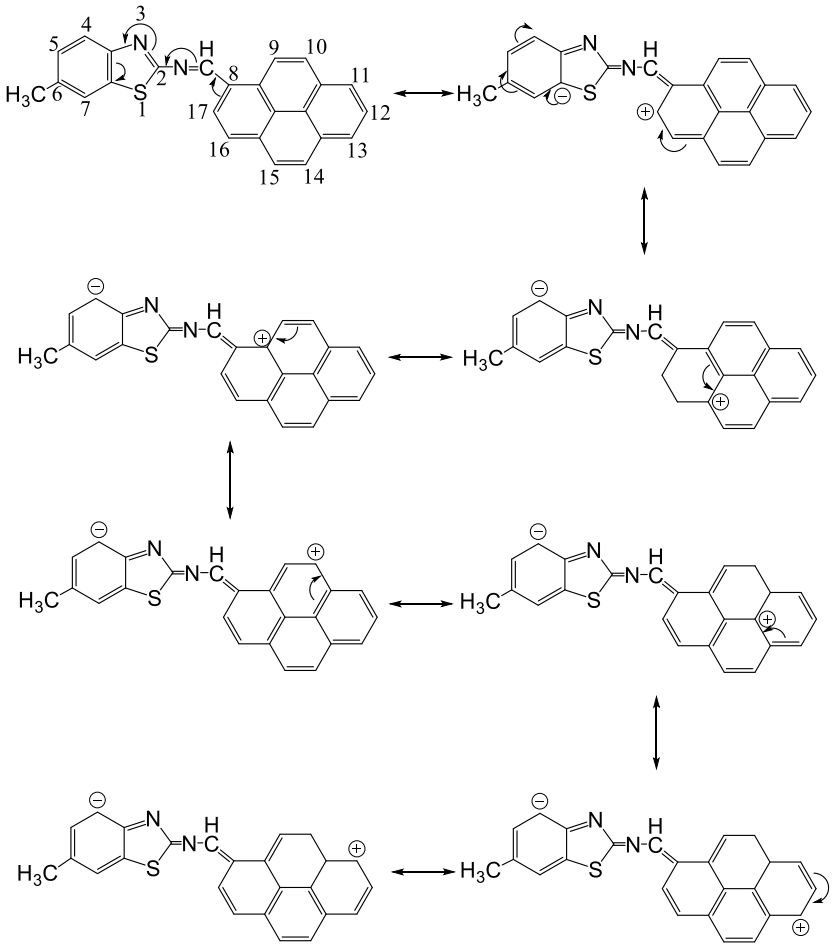

Figure 2. Resonance forms of **3a**

When comparing substance **3b** to substance **3a**, it is observed that its ^{1}H NMR is similar to that of substance **3a**, except for some proton signals (Figure S5). In the resonance structures of compound **3b** (Figure 3), it is observed that the chemical shift values for the protons H6, H10, H11, and H15 of the anthracene ring are higher than those for the protons H7 and H5 of the benzothiazole ring. When the

resonance structures of compound **3c** were examined (Figure 4), it was observed that, as expected, the ^{1}H NMR signals of its protons were similar to the ^{1}H NMR signals of the protons of compounds **3a** and **3b. (**Figure. S6)

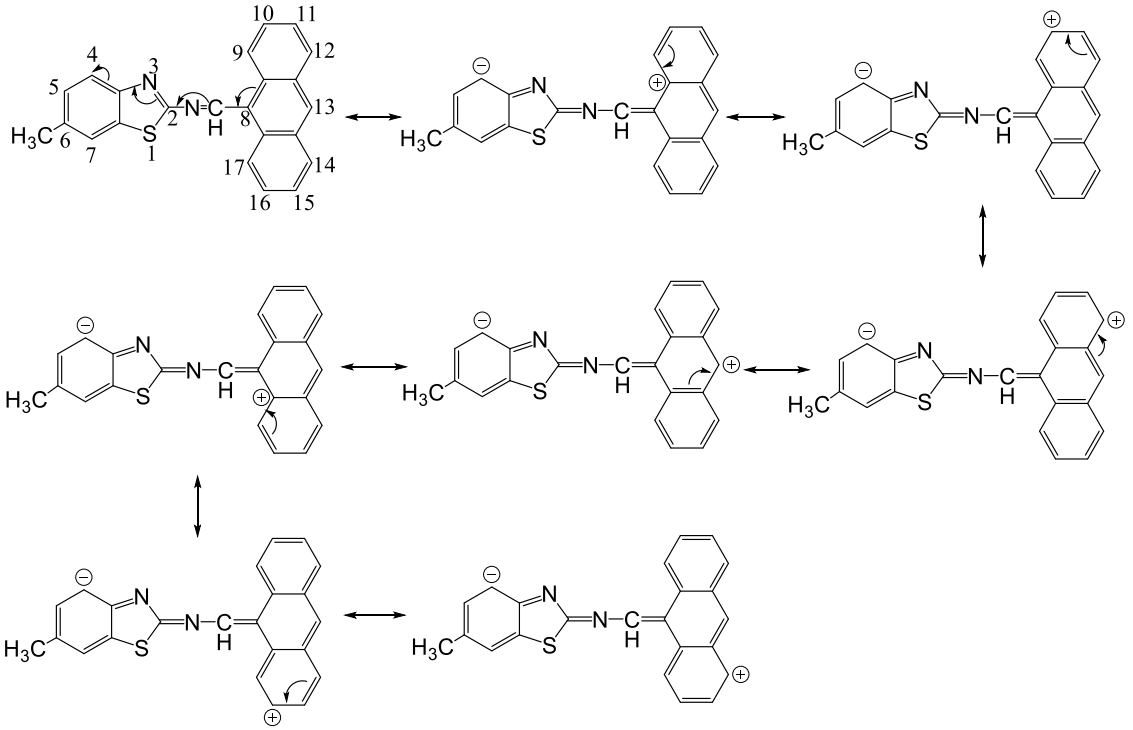

Figure 3. Resonance forms of **3b**

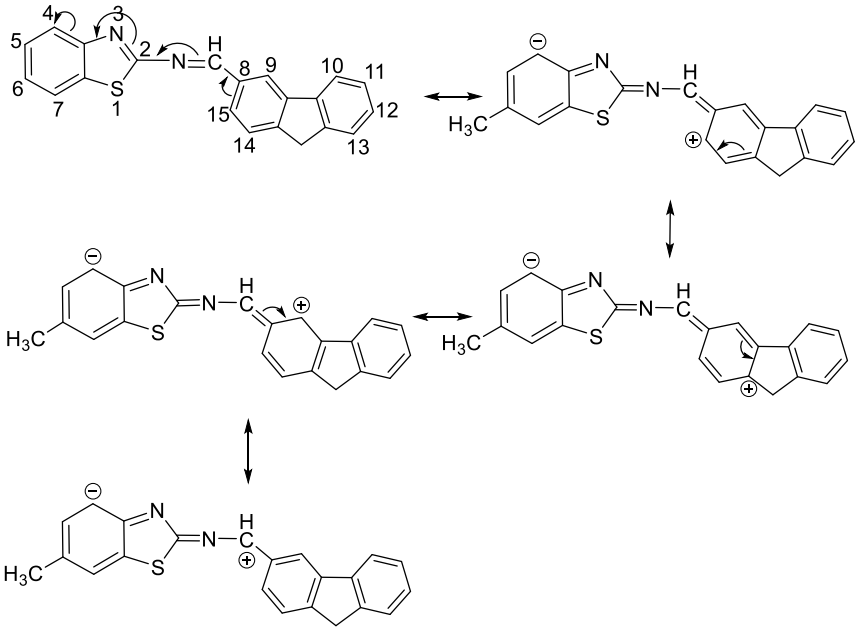

Figure 4. Resonance forms of **3c**

To obtain the ultraviolet-visible spectra of Schiff bases, solutions of Schiff bases (**3a**, **3b,** and **3c**) were prepared at a concentration of 10^{-5} M in n-Hexane, THF, DCM, DMF, DMSO and their absorption

spectra were recorded to elucidate their optical properties. In the UV/vis spectra of Schiff bases (**3a**, **3b,** and **3c**), two transition species belonging to the azomethine group (-CH=N-), namely $n - \pi^*$ and $\pi - \pi^*$ were expected to be observed. π-electron conjugation, also referred to as the π-π* electronic transition, causes the short-wavelength band. Figures 5, 6, and 7 demonstrate that long-wavelength transitions are n-π* transitions resulting from solute-solvent interactions. The substituent methyl in the benzothiazole ring is not indicated in the figure, as it does not contribute to resonance.

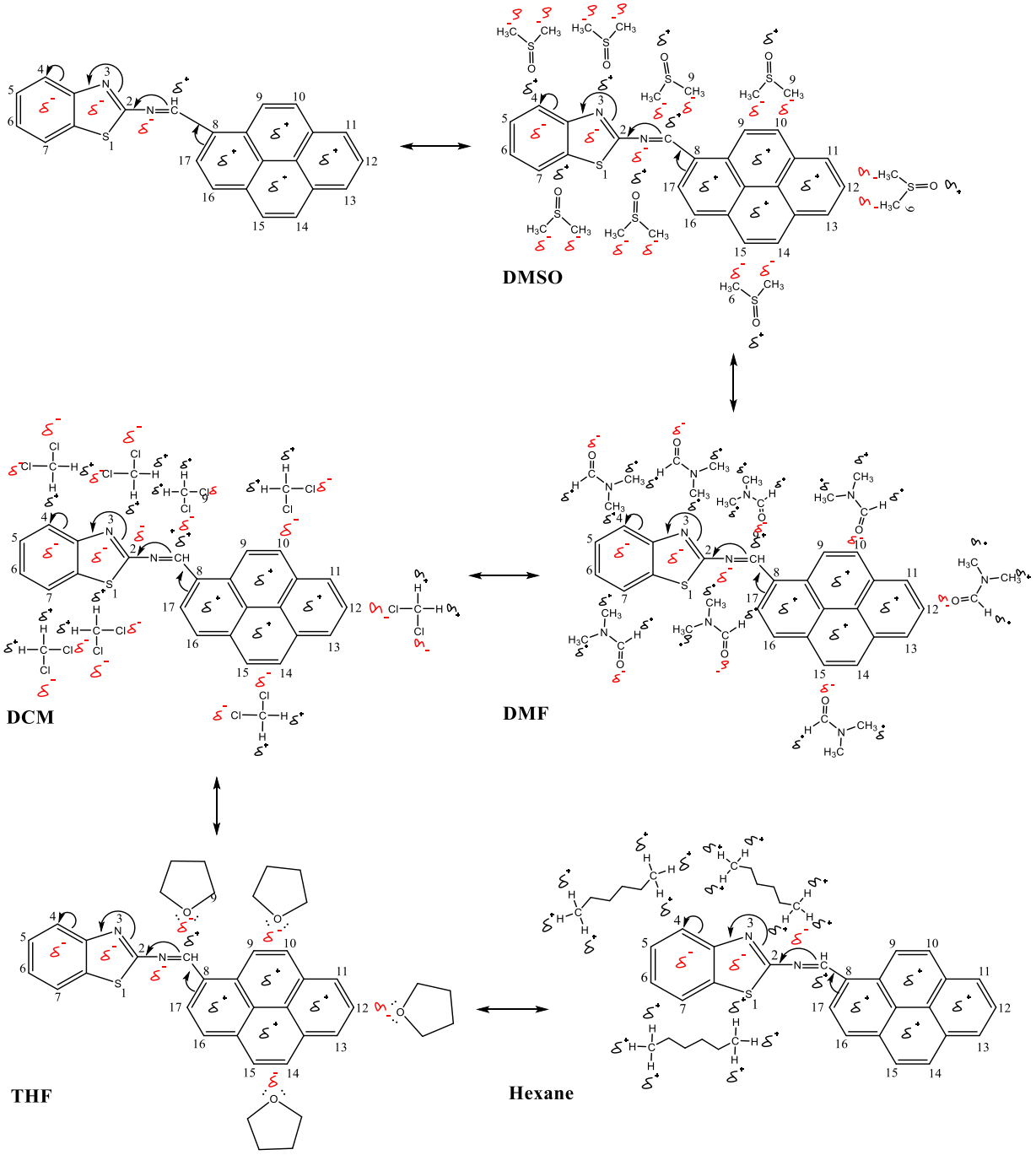

Figure 5. Resonance structures of **3a** in DMSO, DCM, DMF, THF and Hexane

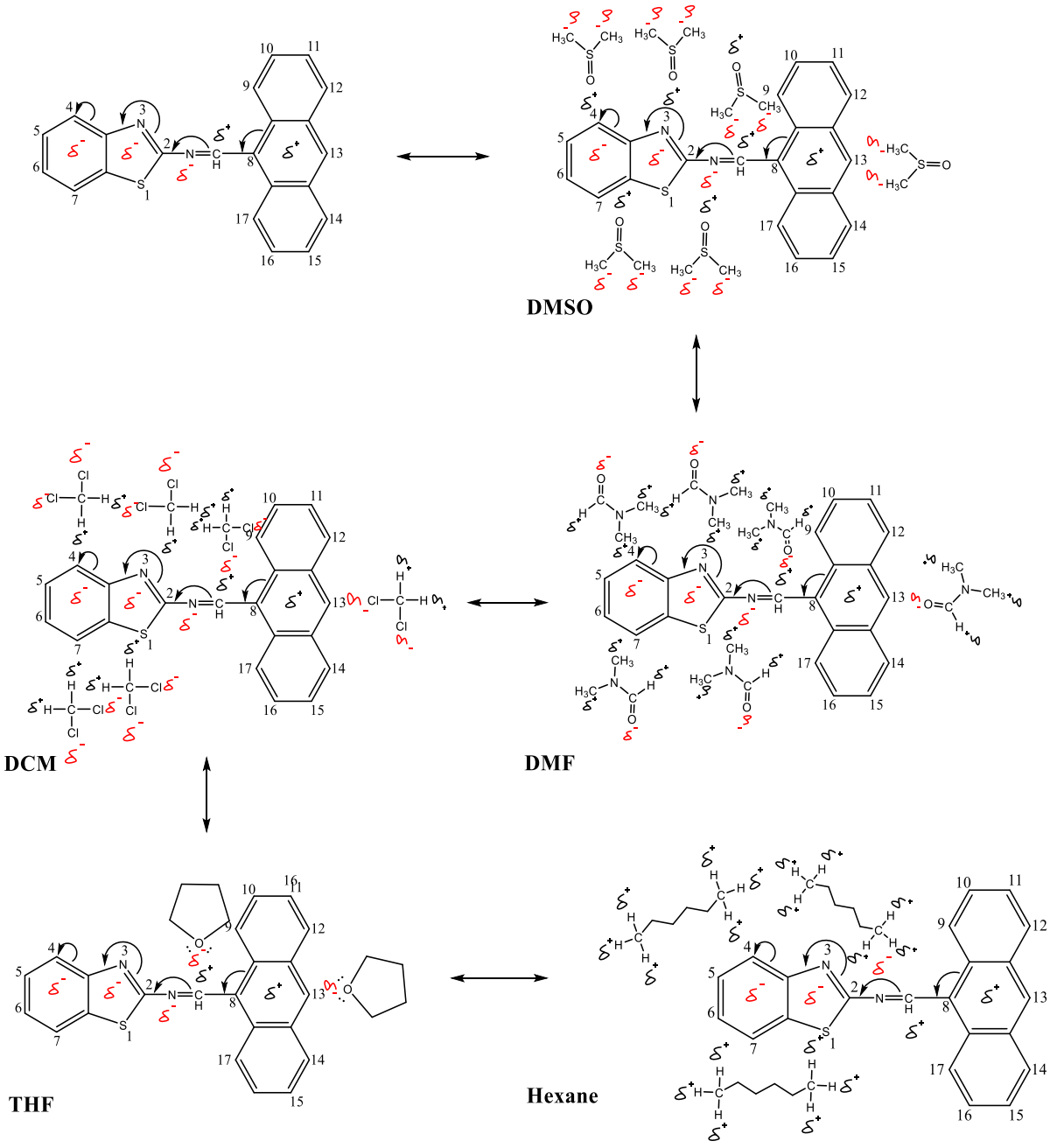

Figure 6. Resonance structures of **3b** in DMSO, DCM, DMF, THF and Hexane

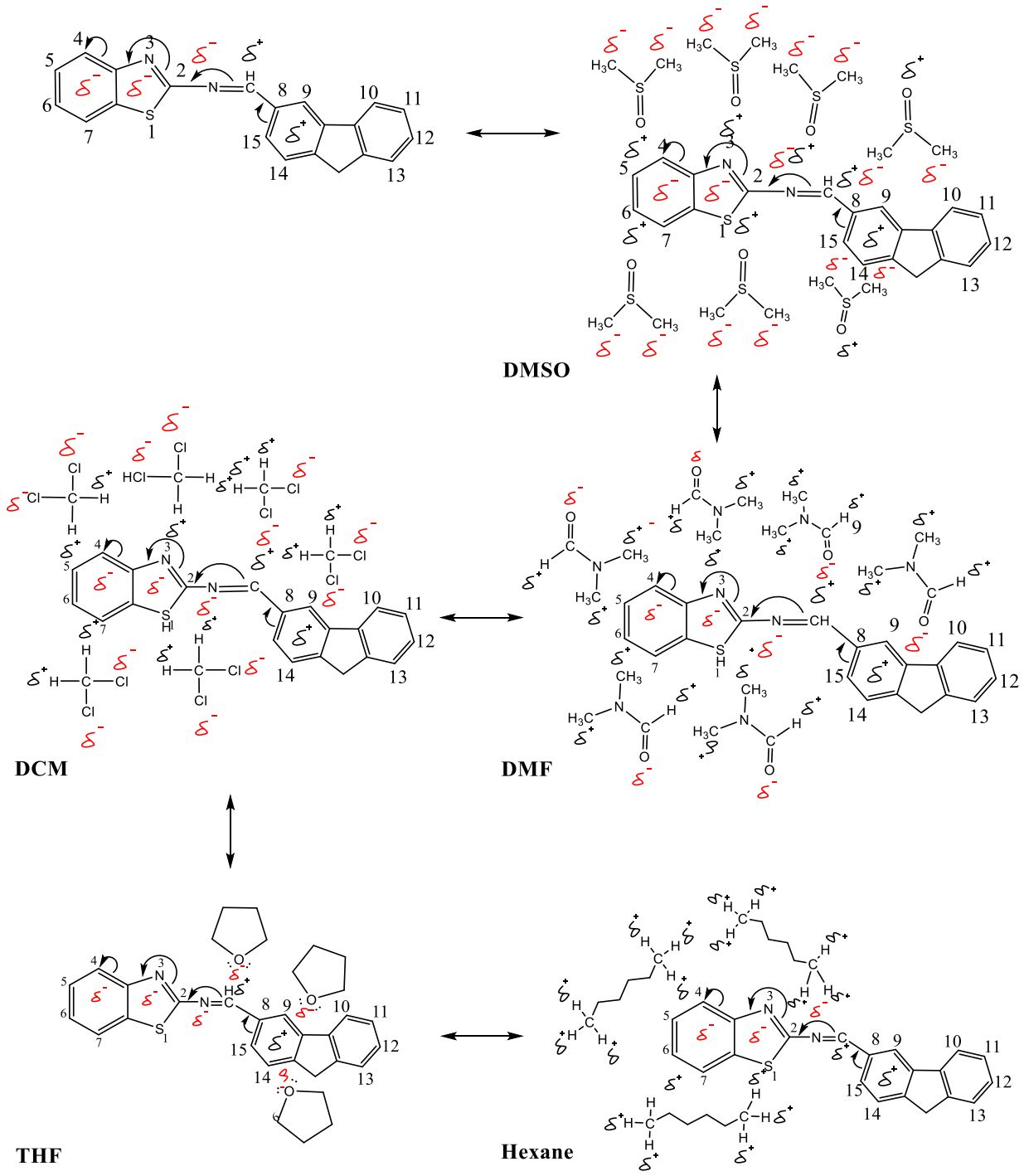

Figure 7. Resonance structures of **3c** in DMSO, DCM, DMF, THF and Hexane

In the UV and visible region spectra of synthesized compounds **3a, 3b**, and **3c**, the λ_{max} value of the $\pi - \pi^*$ transition of the azomethine group of **3a** is 297 nm in hexane solvent and 302 nm in DMSO solvent (Figure. S7). The $\pi - \pi^*$ transition was observed at 270 and 274 nm for compound **3b**, and at 230 nm and 255 nm for compound **3c** (Figure. S8 and S9). However, the $n - \pi^*$ transition of the azomethine group of the same compounds was observed at 421-433 nm for compound **3a**, 437-449 nm for compound **3b** and 367-381 nm for compound **3c** (Table 1). The λmax values of compounds **3a** and **3b** in solvents

of different polarity are red-shifted due to the increase in polarity of the solvent, but this effect is not felt much in compound **3c** due to the lack of conjugation in the fluorene group.

Table 1. The λ_{max} values corresponding to n-π* and π-π* transitions for 3a, 3b, and 3c were measured across various solvents.

	λ_{max} (nm)	n-Hexane	THF	DCM	DMF	DMSO
3a	n-π*	421	427	429	430	433
	π-π*	297	300	300	300	302
3b	n-π*	437	445	446	446	449
	π-π*	270	272	273	264	274
3c	n-π*	367	375	380	378	381
	π-π*	230	233	226	267	255

In compounds **3a** and **3b**, due to the mesomeric effect, which is the distribution of π- electrons on the molecule, the energy of the azomethine's π orbital decreases, and the wavelength increases due to its interaction with polar solvents, thus the $\pi - \pi^*$ transition of the azomethine group shifts to the red. Conversely, in the $n - \pi^*$ transition, the benzothiazole and pyrene rings of the Schiff base (**3a** and **3b**) inductively donate electrons to the azomethine group. This effect is particularly notable in polar solvents, where the energy of the n orbital in the excited state increases as the interaction and polarization between the solute and solvent decrease. As a result, a red shift is observed in the $n - \pi^*$ transition. In compound **3c**, in addition to the above effects, conjugation is removed, and there is a decrease in the wavelength of both the $\pi - \pi^*$ transition and the $n - \pi^*$ transition.

3. COMPUTATIONAL STUDY

Density Functional Theory (DFT) and Time-Dependent Density Functional Theory (TD-DFT) calculations were performed to analyze conformations, obtain thermodynamic data, and investigate the optical properties of new Schiff bases. Much research confirms that DFT calculations provide insight into conjugated molecules' structural and electronic features. TD-DFT is especially useful for reliably simulating molecular structures and spectroscopic properties. This method is primarily used to calculate the excited-state properties of molecules, solids, and nanomaterials, including transition dipole moments, oscillator strengths, and electronic excitation energies. It is a popular tool for simulating UV-Vis, IR, and fluorescence spectra, enabling comparison with experimental data.[27] It is particularly effective at accurately estimating electron distribution and energy levels in conjugated systems. Since the Becke-3 Parameter Lee–Yang–Parr (B3LYP) Correlation [28,29] method and 6-31 G (d,p) basis set are compatible with experimental data; they are primarily utilized in quantum chemical computations of Schiff bases.

Using the Gaussian09 software [30], the ground state optimizations of compounds **3a**, **3b**, and **3c** were carried out in this manner in the gas phase and dimethyl sulfoxide (DMSO) at the B3LYP/6-31 G (d,p) level without any symmetry constraints. The optimization process began with a scan of the Potential Energy Surface (PES) and the selection of the geometry enclosing zero. Vibration frequency calculations were conducted at the same level using B3LYP optimization. By analyzing the harmonic vibrational frequencies using analytical second derivatives with the number of imaginary frequencies (NIMAG), the minima of the computed structures (NIMAG=0) were verified.

Employing the conductor-like polarizable continuum model (CPCM), the solvent effect in DMSO was identified [31, 32]. Gausview was used to conclude the generation of frontier molecular orbitals (FMO). [33]

When the dihedral angles of the molecules in the series are examined, it is seen that the benzothiazole moiety and other fused rings are planar to each other, which is consistent with the expected behavior of a conjugated π-system. Such planarity facilitates effective π-electron delocalization. In contrast, non-planar conformations would reduce the overlap between adjacent π-orbitals, disrupting conjugation, which could lead to increased band gap energy, blue-shifted absorption, and diminished nonlinear optical (NLO) responses. If we examine compound **3a** to imagine the planarity, we can see that the dihedral angle between the pyrene and the benzothiazole plane is approximately 179°. All other dihedral angles around the azomethine bond are given in the supplementary information. Frontier Molecular Orbitals (FMO) were computed to better comprehend the compounds' intramolecular charge transfer (ICT) characteristics.

In compounds **3a**, **3b**, and **3c**, the HOMOs appeared to be localized on the fused rings, azomethine bonds, and benzothiazole. The localization of the LUMOs was observed on the azomethine bonds, with the rings spreading moderately through the benzothiazole (Figure 8). The compounds' λ_{max} values and vertical excitation energies were estimated using the time-dependent DFT (TD-DFT) approach. N states of 50 for singlets were computed to obtain absorption bands. Compounds **3a**, **3b**, and **3c** are predicted to have computed λ_{max} values of 469, 509, and 540 nm in DMSO, indicating low-energy transitions caused by FMO (96-99%). The trends of increasing or decreasing excitation and absorption energies in the estimated and empirically acquired data are consistent. λ_{max} values calculated (in the gas phase and DMSO) and experimentally recorded (DMSO) are given in Table 2. In our previous research, the band gap energies of compounds bearing a 4-methyl-substituted benzothiazole core were calculated using the B3LYP/6-31G(d,p) method and found to be 2.87 eV and 3.19 eV, respectively [26]. In the present study, the same method was applied to the newly synthesized Schiff bases containing a 6-methyl-substituted benzothiazole moiety. The calculated band gap energies of compounds 3a and 3c were determined to be 2.64 eV and 3.02 eV, respectively [26].

The comparison between the previously studied 4-methyl-substituted benzothiazole derivatives and the 6-methyl-substituted Schiff bases presented in this work suggests that the position of the methyl group influences the electronic and optical properties. Specifically, the 6-methyl derivatives (compounds 3a and 3c) exhibit slightly lower band gap energies than their 4-methyl counterparts, indicating enhanced π-electron delocalization and improved intramolecular charge transfer. This shift may be attributed to the altered electron-donating effect and spatial orientation of the methyl group on the conjugated system.

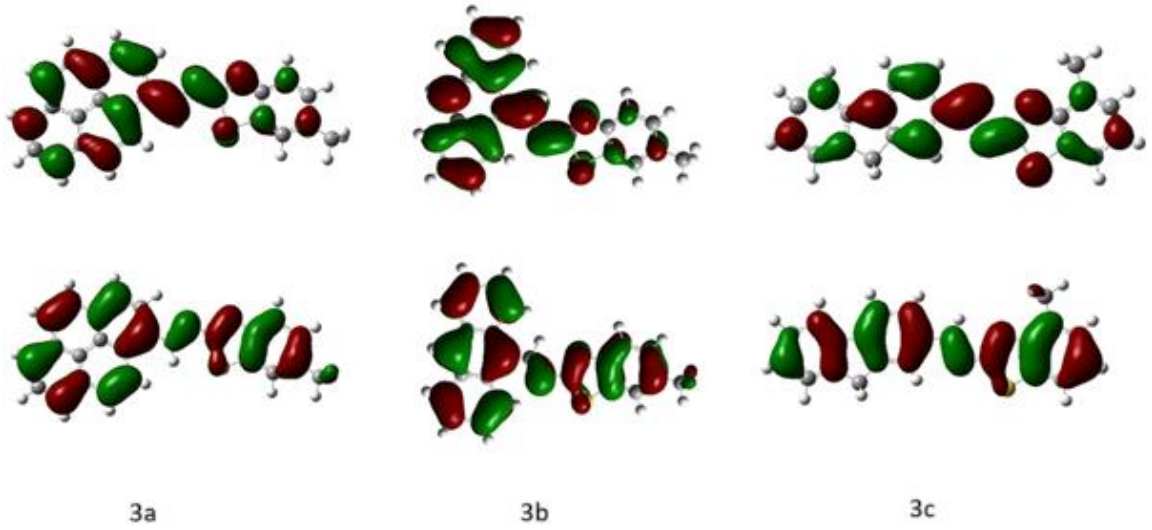

Figure 8. HOMOs and LUMOs of **4** (left), **5** (middle), and **6** (right) estimated at the B3LYP/6-31 G (d, p) level in the gas phase.

Table 2. Calculated and experimental λ_{max} and band gap energies of compounds 3a, 3b, and 3c

Compound	Calculated				Experimental	
	Gas		DMSO		DMSO	
	λ_{max}	Eg	λ_{max}	Eg	λmax	Eg
3a	437	2.84	469	2.64	509	2.44
3b	478	2.59	496	2.5	540	2.29
3c	383	3.24	411	3.02	455	2.73

While the Multiwfn 3.3.8 [34] program performed the NLO computations, VMD 1.9.3 [35]was used to evaluate the hyperpolarizability data. The following equations are essential for calculating the NLO properties. In this context, μ stands for the total dipole moment, α represents isotropic polarizability, Δα refers to polarizability anisotropy, and β indicates static first hyperpolarizability. [36]Understanding these parameters is crucial for accurately assessing the behavior of materials under nonlinear optical conditions.

$$\mu = \left(\mu_x^2 + \mu_y^2 + \mu_z^2\right)^{1/2} \tag{1}$$

$$\alpha = \frac{1}{3}(\alpha_{XX} + \alpha_{XX} + \alpha_{XX}) \tag{2}$$

$$\Delta\alpha = \frac{1}{2}\left\{\left(\alpha_{xx} - \alpha_{yy}\right)^2 + \left(\alpha_{yy} - \alpha_{zz}\right)^2 + (\alpha_{zz} + \alpha_{xx})^2\right\}^{1/2} \tag{3}$$

$$\beta = \left(\beta_x^2 + \beta_y^2 + \beta_z^2\right)^{1/2} \tag{4}$$

Moreover, urea is one of the standard compounds utilized to investigate the NLO characteristics of molecular systems [36, 37]. It has been widely employed as a threshold number for comparative analysis. The calculated values of dipole moment for compounds **3a**, **3b**, and **3c** are 4.8 D, 1.1 D, and 1,4 D, respectively, and compound **3a** is approximately four times the value for urea (1.3732 D) [39]. Polarizability is determined by two factors: molecular size and the number of electrons. It's worth noting that the expansion of atomic size leads to an increase in polarizability, underscoring the close correlation between molecule size and polarizability. The polarizability values for compounds **3a**, **3b**, and **3c** are 609.7 a.u., 384.9 a.u., and 496.6 a.u., respectively. The anisotropy of the polarizability values equals 887.6 a.u., 519.9 a.u., and 712.9 a.u, correspondingly. Based on the findings, the polarizability and anisotropy of compound **3a** are greater than the other compounds. Polarizability and anisotropy also directly correlate with the dipole moment. Hyperpolarizability plays a crucial role in the NLO system. The first hyperpolarizability values for compounds **3a**, **3b**, and **3c** in DMSO are computed to be 4379.6 a.u., 7261.4 a.u., and 7434.4 a.u., respectively. These values are roughly 110.22, 182.75, and 187.104 times greater than the measured value for urea (39.734 a.u.) [37, 38]. These results highlight the significant enhancement in NLO response relative to common benchmark compounds. Urea, often used as a standard reference, has a first hyperpolarizability of approximately 39.7 a.u., whereas the Schiff bases reported here exhibit values more than 100–180 times higher. Compared to other organic materials reported in the literature, such as MDMABA ($\beta \approx 850$ a.u.) and certain azomethine derivatives (typically $\beta < 2000$ a.u.) [15–18], compounds 3b and 3c demonstrate exceptionally strong NLO behavior. This

enhancement is directly correlated with their extended π-conjugation and optimized molecular geometry, which promote efficient intramolecular charge transfer. The combination of high β values and stable molecular structures makes these Schiff bases strong candidates for application in NLO-based technologies such as frequency doubling, optical switching, and electro-optic modulation.

4. EXPERIMENTAL

Chemicals were acquired from Sigma-Aldrich and used without additional purification. The organic solvents were of HPLC grade or purified by a standard procedure, and the FT-IR and UV-visible absorption spectroscopy were collected at the Inorganic Chemistry Research Laboratory of Eskisehir Osmangazi University. FT-IR spectra were obtained using a Bruker FT-IR spectrometer within the 4000-400 cm^{-1} wavelength region. UV-visible absorption spectrum was obtained using a SHIMADZU UV-2600 spectrometer. The Gallenkamp melting point apparatus was used to determine the melting points. At the University Central Research Laboratory in Ankara, ESI-MS and elemental analysis were conducted using the Waters Alliance HPLC, 2Q micro mass spectrometer, and Leco CHNS 932 Elemental Analyzer. Thin-layer chromatography (TLC) plates were acquired pre-coated from MERCK and utilized for reaction monitoring ^{1}H NMR (500 MHz, DMSO-d6, TMS internal standard) and ^{13}C NMR (125 MHz, DMSO-d6, TMS internal standard) spectroscopic investigations were conducted by Jeol ECZ500R (11.75 Tesla) NMR instrumentation at the Eskisehir Osmangazi University Central Research Laboratory Application and Research Center (ARUM). In Ankara, University Central Research Laboratory, ESI-Mass and elemental analyses were recorded by Waters Alliance HPLC, a 2Q micro mass spectrometer, and Leco CHNS 932 Elemental Analyzer. The computational process, advancing from simple to complex, involved both molecular mechanics and quantum chemical calculations performed on a desktop computer equipped with an Intel Core i7 Extreme 3970x 3.50 GHz six-core twelve-thread processor, 64GB (8x8GB) DDR3 1333 MHz RAM, and an Intel x79 chipset LGA2011 socket. Density Functional Theory computations were conducted with the Gaussian 09 software package.

Compounds 3a, 3b, and 3c *(General procedure)*. A solution of 6-methyl-2-amino benzothiazole (**2**, 0.3 g, 1.83 mmol) in ethyl alcohol (10 mL) was combined with pyrene carbaldehyde, 9-anthracene carbaldehyde, or fluorene-2-carbaldehyde (**1**, 0.34 g, 1.46 mmol). Two to three drops of a 5% hydrochloric acid solution were introduced into the reaction media and subjected to reflux under a nitrogen environment at 75°C for four hours. The TLC control halted the reaction (1:10 Petroleum ether / DCM). After overnight cooling the solution at ambient temperature, the precipitates were filtered and extracted using DCM and recrystallized from ethyl alcohol. Compounds **3a**, **3b**, and **3c** were synthesized with yields of 44%, 82%, and 43%, respectively. The procedure for synthesizing the **3a**, **3b**, and **3c** Schiff bases, together with the proton numbering in the molecule, is encapsulated in Figure 1.

N-(6-methylbenzo[d]thiazol-2-yl)-1-(pyren-1-yl) methinamine (3a). Yield 44%, yellow solid, mp 203-205 ºC. IR spectrum (KBr), ν, cm^{-1}: 3040 (Aromatic C-H), 2910 and 2851 (Aliphatic C-H), 1586 (CH=N), 1564, 1527 and 1440 (C=C) (Figure. S1). ^{1}H NMR spectrum, δ, ppm: 10,03 s (1H, -CH=N-), 9.29 d (1H, *J* 10 Hz, H17), 8.84 d (1H, *J* 8 Hz, H10), 8.43 m (4H, H11, H13, H14, H9), 8.39 d (1H, *J* 8 Hz, H16), 8.28 d (1H, *J* 8 Hz, H15), 8.16 t (1H, *J* 8 Hz, H12), 7.86 t (2H, *J* 9 Hz, H5 and H7), 7.34 d (1H, *J* 9 Hz, H4), 2.4 s (3H, CH_3) (Figure. S4) ^{13}C NMR spectrum, δ_C, ppm: 135.0 (CH=N), 133.25, 131.82, 131.32, 130.11, 130.79, 130.67, 130.42, 128.17, 126.10, 126.56, 126.49, 126.40, 126.32, 125.76, 123.42, 122.89, 122.58, 121.45. Mass spectrum, m/z (I, rel. %). 377.68 (M^+), 378.71 (M^++1), 379.77 (M^++2), 245.48 (M^+ -$C_8H_8N_2S$), 165.15 (M^+ -$C_{17}H_{19}$). Found, %: C 79.52; H 4.44; N 7.37; S 8.40, $C_{25}H_{16}N_2S$ Calculated, %: C 79.76; H 4.28; N 7.44; S 8.52.

1-(anthracen-9-yl)-N-(6-methylbenzo[d]thiazol-2-yl) methinamine (3b). Yield 82%, yellow solid, mp 207-211 ºC. IR spectrum (KBr), ν, cm^{-1}: 3042 (Aromatic C-H), 2915 (Aliphatic C-H), 1549 (CH=N), 1515, 1478 and 1436 (C=C) (Figure. S2). ^{1}H NMR spectrum, δ, ppm: 10.32 s (1H, -CH=N-), 9.01 d

(2H, *J* 9 Hz, H9, H17), 8.94 s (1H, H13), 8.21 d (2H, *J* 8 Hz, H12 and H14), 7.87 d, s (2H, *J* 8 Hz, H7 and H5), 7.73 dt (2H, *J* 3 Hz, *J* 8 Hz, H16 and H10), 7.63 t (2H, *J* 7 Hz, H11 and H15), 7.33 dd (1H, J=1 Hz, *J* 8 Hz, H4), 2.6 s (3H, CH_3) (Figure.S5). Mass spectrum, m/z (I, rel. %). 353,65 (M^+), 354,32 (M^++1), 355,64 (M^++2), 165,43 (M^+ -$C_{15}H_{19}$).

1-(9H-fluoren-2-yl)-N-(6-methylbenzo[d]thiazol-2-yl) methinamine (3c). Yield 43%, brown solid, mp 189-201 ºC. IR spectrum (KBr), ν, cm^{-1}: 3023 (Aromatic C-H), 2963 and 2909 (Aliphatic C-H), 1554 (CH=N), 1580, 1556 and 1475 (C=C) (Figure S3). ^{1}H NMR spectrum, δ, ppm: 9.20 s (1H, -CH=N-), 8.26 s (1H, H9), 8.08 s (2H, H14 and H15), 8.00 d (1H, *J* 7 Hz, H13), 7.82 s (1H, H7), 7.79 d (1H, *J* 9 Hz, H10), 7.62 d (1H, *J* 8 Hz, H5), 7.41 dt (2H, *J* 1 Hz, *J* 7 Hz, H11 and H12), 7.30 dd (1H, *J* 3 Hz, *J* 7 Hz, H4), 4.00 s (2H, Fluoren –CH_2), 2.43 s (3H, CH_3) (Fig.S6). Mass spectrum, m/z (I, rel. %).341,63 (M^+), 342,57 (M^++1), 343,65 (M^++2), 209,41 (M^+ -$C_{15}H_{13}$), 165,21 (M^+ -$C_{14}H_{10}$).

5. CONCLUSION

This study focused on the synthesis, characterization and computer-aided calculations of three new Schiff bases named compounds **3a**, **3b** and **3c.** The band gap energies were taken in DMSO solvent using UV-visible absorption spectrophotometry and the optical band gaps of compounds 3a, 3b and 3c were found to be 2.44 eV, 2.29 eV and 2.73 eV, respectively.

According to the data, compound **3a** demonstrates higher polarizability and anisotropy than the other compounds. As previously mentioned, hyperpolarizability is crucial in nonlinear optical (NLO) systems. The computed initial hyperpolarizability values for compounds **3a**, **3b**, and **3c** in DMSO are 4379.6 a.u., 7261.4 a.u., and 7434.4 a.u., respectively. These values are approximately 110.22, 182.75, and 187.10 times larger than the observed value for urea, which is 39.734 a.u. Furthermore, no significant correlation was found between the estimated and experimentally determined band gap energies and hyperpolarization data.

These results demonstrate that Schiff bases 3a, 3b, and 3c exhibit promising nonlinear optical (NLO) properties, with first hyperpolarizability values significantly exceeding that of conventional reference compounds such as urea. The combination of experimental findings and DFT-based theoretical analysis confirms that molecular structure and substitution position directly influence the optical band gaps and electronic behavior. Therefore, these π-conjugated Schiff base systems may serve as potential candidates for future photonic and optoelectronic applications requiring strong NLO responses.

ACKNOWLEDGMENT

The authors thank the Eskişehir Osmangazi University Scientific Research Projects Council for financial support (Project No 202019059). We would also like to thank our master's student Sevgi ŞEN from Eskişehir Technical University for her help in the physical arrangement of the manuscript.

CONFLICT OF INTEREST

The authors stated that there are no conflicts of interest regarding the publication of this article.

CRediT AUTHOR STATEMENT

Sultan Funda Ekti: Writing – Review & Editing, Conceptualization, Supervision, Investigation**. Handan Can Sakarya:** Project administration, Investigation, Writing – Review & Editing. **Yunuscan Sivrikaya:** Investigation.

REFERENCES

[1] Marder SR, Organic nonlinear optical materials Where we have been and where we are going, Chemical Communications 2006;37;131-4.

[2] Mehkoom M, Afzal M, Ahmad S, Khan SA. The new pyrazoline derivative 5-(3,4-Dimethoxy-phenyl)-3-(2,5-dimethyl-thiophene-3-yl),-4,5-dihydro-pyrazole-1-carbothioic acid amide (DDPA) as an advisable candidate for optical linearity, nonlinearity, and limiting performance. J Mol Liq 2022;345;117018.

[3] Gong P, Liu X, Kang L, Lin Z. Inorganic planar π-conjugated groups in nonlinear optical crystals: Review and Outlook. Inorganic Chemistry Frontiers 2020;7;839-852.

[4] Evans OR, Lin W. Crystal engineering of NLO materials based on metal-organic coordination networks. Ac Chem Res 2002; 35; 511–522.

[5] Abrinaei F, Kimiagar S, Gharedaghi S. Strong optical nonlinearity of CdS/nitrogen-doped reduced graphene oxide nanocomposites using Z-scan technique. Journal of Materials Science: Materials in Electronics 2018; 29; 2550–2560.

[6] Alamouti AF, Nadafan M, Dehghani Z, Ara MHM, Noghreiyan AV. Structural and Optical Coefficients Investigation of γ-Al2O3 Nanoparticles using Kramers-Kronig Relations and Z–scan Technique. Journal of Asian Ceramic Societies 2021; 9; 366–373.

[7] Dehghani Z, Nadafan M, Saievar IE. The effect of external applied fields on the third order nonlinear susceptibility of ferro-nematics. J Mol Liq 2015; 204; 70–75.

[8] Abrinaei F. Laser ablation of magnesium in water and investigation of optical nonlinearity by the Z-scan technique. Journal of the Optical Society of America B 2016; 33; 864.

[9] Hasmuddin M, Abdullah MM, Singh P, Shkir M, Vijayan N, Wahab MA. Ab-initio study of L-Tartaric Acid (LTA) single crystal for NLO application, Opt Laser Technol 2015; 74; 53–59.

[10] Jagadesan A, Sivakumar N, Mohan KR, Chakkaravarthi G, Arjunan S. Synthesis, crystal structure, growth and characterization of an optical organic material: 4-Aminopyridinium Trichloro acetate single crystal. Opt Mater 2018; 84; 864–869.

[11] Kwon SJ, Jazbinsek M, Kwon OP, Günter P. Crystal Growth and Morphology Control of OH1 Organic Electrooptic Crystals. Cryst Growth Des 2010; 10; 1552–1558.

[12] Sabaa MW, Elzanaty AM, Abdel-Gawad OF, Arafa EG. Synthesis, characterization and antimicrobial activity of Schiff bases modified chitosan-graft-poly(acrylonitrile). Int J Biol Macromol 2017; 109; 1280–1291.

[13] Poonia K, Siddiqui S, Arshad M, Kumar D. In vitro anticancer activities of Schiff base and its lanthanum complex. Spectrochim Acta A Mol Biomol Spectrosc 2016; 155; 146–154.

[14] Inan A, İkiz M, Tayhan SE, Bilgin S, Genç N. Antiproliferative, antioxidant, computational and electrochemical studies of new azo-containing Schiff base ruthenium(II) complexes. New Journal of Chemistry 2018; 42; 2952–2963.

[15] Leela S, Ramamurthi K, Bhagavannarayana G, Synthesis, growth, spectral, thermal, mechanical and optical properties of 4-chloro-4′dimethylamino-benzylidene aniline crystal: A third order nonlinear optical material. Spectrochim Acta A Mol Biomol Spectrosc 2009; 74; 78–83.

[16] Leela S, Hema R, Stoeckli EH, Ramamurthi K, Bhagavannarayana G. Design, synthesis, growth and characterization of 4-methoxy-4′- dimethylamino-benzylidene aniline (MDMABA): A novel third order nonlinear optical material. Spectrochim Acta A Mol Biomol Spectrosc 2010; 77; 927–932.

[17] Leela S, Deepa RT, Subashini A, Brindha S, Ramesh BR, Ramamurthi K. Studies on growth and characterization of nonlinear optical material 4-chloro-4′methoxy benzylideneaniline: A Schiff base organic material. Arabian Journal of Chemistry 2017; 10; S3974–S3981.

[18] Subashini A, Kumaravel R, Leela S, Evans HS, Sastikumar D, Ramamurthi K, Synthesis, growth and characterization of 4-bromo-4′chloro benzylidene aniline - A third order non linear optical material. Spectrochim Acta A Mol Biomol Spectrosc 2011; 78; 935–941.

[19] Subashini A, Bhagavannarayana G, Ramamurthi K. Synthesis, growth, optical, mechanical, dielectric and thermal properties of 4-chloro-4′-chlorobenzylidene aniline single crystal. Spectrochim Acta A Mol Biomol Spectrosc 2011; 82; 91–96.

[20] Czekalla GB. Elektronenuberfuhrung durch Lichtabsorption und-emission in Ele ktronen-Donator-Acceptor-Komplexen. Angewandte Chemie 1960;72;401-413.

[21] Shafiee A, Yahaya M.Determination of HOMO and LUMO of [6,6]-Phenyl C61-butyric Acid 3-ethylthiophene Ester and Poly (3-octyl-thiophene-2, 5-diyl) through Voltametry Characterization (Penentuan HOMO dan LUMO Asid [6,6]-Fenil C61-butirik Ester 3-etiltiofena dan Poli (3-oktil-tiiofena-2, 5-diyl) menerusi Pencirian Voltametri). Sains Malaysiana 2011; 40(2), 173-176.

[22] Runge E, Gross EKU. Density-Functional Theory for Time-Dependent Systems. Phys Rev Lett 1984; 52; 997–1000.

[23] Turkoglu G, Cinar ME, Buyruk A, Tekin E, Mucur SP, Kaya K, Ozturk T. Novel organoboron compounds derived from thieno[3,2-b] thiophene and triphenylamine units for OLED devices. J Mater Chem C Mater 2016; 4; 6045–6053.

[24] Wałęsa Chroab M, Tremblay MH, Skene WG. Hydrogen-Bond and Supramolecular-Contact Mediated Fluorescence Enhancement of Electrochromic Azomethines. Chemistry - A European Journal 2016; 22; 11382–11393.

[25] Salih KSM. Synthesis, characterization, surface analysis, optical activity and solvent effects on the electronic absorptions of Schiff base-functionalized amino thiophene derivatives: Experimental and TD-DFT investigations. J Mol Struct 2021; 1244;131267.

[26] Sıvrıkaya Y, Sakarya HC, Kiliç G, Ektı SF, Yandimoğlu M. New pyrene and fluorene-based π-conjugated Schiff bases: Theoretical and experimental investigation of optical properties. Journal of the Serbian Chemical Society 2024; 89; 1025–1038.

[27] Runge E, Gross EKU. Density-Functional Theory for Time-Dependent Systems. Physical Review Letters 1984;52;12.

[28] Becke AD. Density-functional thermochemistry. III. The role of exact Exchange. J Chem Phys 1993; 98; 5648–5652.

[29] Lee C, Yang W, Parr RG. Development of the Colic-Salvetti correlation-energy formula into a functional of the electron density. Phys Rev B 1988;37;785-789.

[30] Storm AT, Gjikaj M, Namyslo JC, Adams J, Schmidt A. 1,3-Thiazolium-4-aminides: Syntheses and Characterization of Fluorescent Mesoionic Compounds. European J Org Chem 2021; 34; 4803–4815.

[31] Cossi M, Rega N, Scalmani G, Barone V, Energies, Structures, and Electronic Properties of Molecules in Solution with the C-PCM Solvation Model. Comput Chem 2003;24;669-81.

[32] Barone V, Cossi M. Quantum Calculation of Molecular Energies and Energy Gradients in Solution by a Conductor Solvent Model. The Journal of Physical Chemistry A 1998;102;1995-2001.

[33] Underwood SJ, Douglas CJ. N-Pyridylimidates as Traceless Acyl Equivalents for Directed C-O Bond Functionalization. Organic Letters 2023;25;146-151.

[34] Lu T, Chen F. Multiwfn: A multifunctional wavefunction analyzer. J Comput Chem 2012; 33; 580–592.

[35] Humphrey W, Dalke A, Schulten K. VMD: Visual Molecular Dynamics. J Mol Graph 1996;1;33-8.

[36] Williams DJ, DS. Prasad PN. Introduction to Nonlinear Optical Effects in Molecules and Polymers. New York NY, USA;wiley; 1991.

[37] Vennila P, Govindaraju M, Venkatesh G, Kamal C. Molecular structure, vibrational spectral assignments (FT-IR and FT-RAMAN), NMR, NBO, HOMO-LUMO and NLO properties of O-methoxybenzaldehyde based on DFT calculations. J Mol Struct 2016; 1111; 151–156.

[38] Ergürhan O, Gürhan R, Parlak C, Alver Ö. Nonlinear Optical and Spectral Properties Of Hydroquinone & Fullerene Systems. Eskişehir Teknik Üniversitesi Bilim ve Teknoloji Dergisi B - Teorik Bilimler 2021; 9; 47–53.

[39] Abbaz T, Bendjeddou A, Villemin D. Structural and quantum chemical studies on aryl sulfonyl piperazine derivatives. Journal of Drug Delivery and Therapeutics 2019; 9; 88–97.